Chapter

Critical Dry Spell Prediction in Rain-Fed Maize Crop Using Artificial Neural Network in Nigeria

Nnadozie Okonkwo Nnoli, Ahmed Balogun, Jerome Omotosho and Samuel Agele

Abstract

Prediction of yearly mid-growing season first and second critical dry spells using artificial neural networks (ANN) for enhanced maize yield in nine stations in Nigeria is performed. The ANN model uses nine meteorological parameters to predict onset dates and lengths of the critical dry spells. The daily dataset is from 1971 to 2013 of which about 70% is used for training while 30% is for testing. Seven ANN models are developed for each station with a view to measuring their predictive ability by comparing predicted values with the observed ones. Prediction lead times for the two critical dry spell onset dates generally range from about 2 weeks to 2 months for the nine stations. Error range during testing for the onset dates and lengths of first and second critical dry spells is generally ±4 days. The root-mean-square error (RMSE), coefficient of determination, Nash-Sutcliffe coefficient of efficiency, Wilmott's index of agreement, and RMSE observation standard deviation ratio range from 0.46 to 3.31, 0.58 to 0.93, 0.51 to 0.90, 0.82 to 0.95, and 0.30 to 0.69, respectively. These results show ANN capability of making the above reliable predictions for yearly supplementary irrigation planning, scheduling, and various other decision makings related to sustainable agricultural operations for improved rain-fed maize crop yield in Nigeria.

Keywords: Nigeria, rain-fed maize, critical dry spells, yearly prediction, artificial neural network

1. Introduction

Variability of rainfall in Nigeria as well as in West Africa, etc., leads to the occurrence of wet and dry spells within the growing season. Short- and long-duration dry spells are noted during the period of crop growth and development on yearly basis. Song et al. [1] using weather- and county-level maize yield data estimated the drought risk for maize in China for the period from 1971 to 2010. They noted that drought risk had increased in China over the last 40 years and that the reasons for the observed changes were increased drought hazard associated with climate change and increased exposure of maize to drought due to an expanded production area. Significant drought incidents have seriously affected sustainable agriculture, people's living condition, and the economy of many developing and under-developed countries [2, 3]. The occurrence and distribution of dry spells, especially the longer ones at critical times during growing season, generally have negative impact on maize crop development and yield under rain-fed farming in Nigeria. According to Mugalavai et al. [4] and Gao et al. [5], the most critical growth stages for maize crop in terms of dry spell occurrences are the germination, tasseling, and flowering. Germination is within the initial stage, while tasseling and flowering occur during the mid-season stage of growing season. The four crop growth stages are initial, development, mid-season, and late season [6]. Advance knowledge on critical dry spell onset dates and lengths for rain-fed maize crop on yearly basis is very important in supplementary irrigation planning, scheduling, and various other decision makings related to sustainable agricultural operations for improved maize yield.

Sharma [7] noted that a major challenge of drought research was to develop suitable methods and techniques for forecasting the onset and termination points of droughts. Successful development of suitable methods will enable stakeholders in agricultural and water resource sectors of the economy to embark upon risk-based (proactive) rather than crisis-based (reactive) approach to drought management in areas prone to drought [8, 9]. This is also applicable to dry spell management. Most publications are concerned with probabilistic, statistical, and stochastic modeling, and the most widely used stochastic models are autoregressive integrated moving average (ARIMA) models [10]. A dynamical model and a statistical model have been used to determine trends and make seasonal predictions of rainfall and dry spells occurrence in Ghana [11].

In recent years, neural-based models have been gaining attention over statistical models, possibly owing to the simplicity in modeling complex problems when many parameters are taken into consideration [12]. Abrishami et al. [13] used artificial neural network (ANN) model for estimating wheat and maize daily standard evapotranspiration. The results showed the suitable capability and acceptable accuracy of ANN. Mulualem and Liou [14] developed seven ANN predictive models incorporating hydro-meteorological, climate, sea surface temperatures, and topographic attributes to forecast the standardized precipitation evapotranspiration index (SPEI) for seven stations in the Upper Blue Nile basin (UBN) of Ethiopia from 1986 to 2015. Statistical comparisons of the different models showed that accurate results in predicting SPEI values could be achieved by including large-scale climate indices. Morid et al. [15] were able to show the efficiency of ANN when it was used for forecasting some drought indices in some selected places in Iran for up to 12 months lead times [3]. One neural network model was developed to forecast precipitation occurrences such as "rain" or "no-rain," while another model was developed to predict the amount of precipitation at several sub-levels using fuzzy techniques in Sri Lanka [16]. The ability of neural network model to predict "no-rain" situation gives it credence to forecast dry spell. Mathugama and Peiris [17] therefore recommended the exploration of the use of artificial neural network (ANN) to predict dry spell properties and that the models had to be statistically validated. Studies related to forecasting critical dry spell onset dates and lengths (especially mid-growing season dry spells) in Nigeria and other places are scarce. Farmers (especially maize farmers) in Nigeria desire to know on yearly basis when dry spells—critical dry spells—will occur after planting their crops to enable them plan their yearly agricultural operations effectively. In Nigerian Meteorological Agency (NiMet), numerical model have been used for sub-seasonal to seasonal forecasts of weather elements [18], while statistical models are used in seasonal rainfall forecasts for agricultural activities. Probabilistic forecasts have been made [19] for severe dry spell occurrences of lengths 10–21 days and moderate ones of lengths 8–15 days for 10 northern States for the month of June for year 2020; however, specific dry spells onset dates are not given.

These informed our embarking on this study in aid of effective yearly agricultural operations for improved crop yield and maize in particular. The objective therefore of the present work is to predict the onset dates and lengths of mid-growing season critical dry spells for rain-fed maize crop *on yearly basis* in Nigeria using artificial neural network (ANN) model to enable farmers in those stations plan *yearly* agricultural operations for enhanced maize yield.

2. Study area, data, and methodology

2.1 Study area

Table 1 shows the geographical and some climate characteristics of the study area. The following nine meteorological stations in their respective agro-ecological zones in Nigeria are considered: Calabar, Warri, Ibadan, Makurdi, Lokoja, Ilorin, Yola, Kaduna, and Yelwa.

2.2 Data

a. The data used for this work are as follows: the daily maximum, minimum, and mean temperatures, 0600 and 1500 GMT relative humidity, wind speed at 2 meter level, and sunshine hours (1971–2013) for the nine stations from Nigerian Meteorological Agency (NiMet), Oshodi, Lagos and supplemented with 0.125° resolution ERA INTERIM Reanalysis data (1979–2013) [20].

b. NiMet daily rainfall data supplemented with the daily 0.25° horizontal resolution 3B42 rainfall from Tropical Rainfall Measuring Mission (1998–2013) [21].

Since the NiMet data were supplemented as stated above, the Adapted Caussinus-Mestre Algorithm for homogenizing Networks of Temperature series (ACMANT) was used to check and correct the inhomogeneities in the quality controlled time series. A full scientific description of ACMANT setup could be found in [22]. Several studies included [22, 23], etc. have been effectively used ACMANT in homogenizing series. Good performances of homogenizing climatic series with ACMANT are noted in the result evaluation from these studies.

Agro-ecological zone	Station	Long.	Lat.	Elev. (m)	Annual rainfall (mm/year) (1971–2013)		
					Max.	Min.	Mean
Northern Guinea Savannah	Yelwa	4.75°E	10.88°N	244.0	1564.6	388.9	986.5
	Kaduna	7.45°E	10.60°N	641.0	1659.8	793.4	1211.1
	Yola	12.47°E	9.23°N	190.5	1142.7	468.5	873.4
Southern Guinea Savannah	Ilorin	4.58°E	8.48°N	344.0	1539.3	697.7	1177.6
	Lokoja	6.73°E	7.80°N	62.5	1767.1	771.7	1196.4
	Makurdi	8.53°E	7.75°N	91.4	1617.1	761.5	1182.8
Rain Forest	Ibadan	3.90°E	7.43°N	220.7	1967.8	775.7	1328.9
Mangrove Swamp	Warri	5.73°E	5.52°N	6.0	3414.4	2051.5	2734.3
	Calabar	8.33°E	4.95°N	62.3	4044.9	2109.5	2937.6

Table 1.
Area of study showing the stations, agro-ecological zones and climate characteristics.

2.3 Methodology

2.3.1 Growing season onset and cessation dates

The determination of onset and cessation dates of growing season was carried out using the methods of [24, 25]. The onset date of growing season was defined by [24] for northern Nigeria as the date when accumulated daily rainfall exceeded 0.5 of the accumulated reference evapotranspiration for the remainder of the season, provided that no dry spell of 5 days or more occurred in the week after that date. The determination of onset date of rains according to [25] was from the first point of maximum positive curvature of the plotted graph of cumulative percentage of pentade rainfall, while cessation was from the last point of maximum negative curvature of the plotted graph of cumulative percentage of pentade rainfall. The method of [25] was initially used to determine the onset dates of growing season, while that of [24] was next used to ensure that no dry spell of 5 days or more occurred in the week after that date.

2.3.2 Reference evapotranspiration

To determine the critical dry spells during each growing season, the daily reference evapotranspiration (ET_o) was first computed using the FAO Penman-Monteith Equation [6]. This equation, given below (Eq. (1)), used the abovementioned data with the exception of daily rainfall.

$$ET_o = \frac{0.408\Delta(R_n - G) + \gamma\left(\frac{900}{T+273}\right)u_2(e_s - e_a)}{\Delta + \gamma(1 + 0.34u_2)} \tag{1}$$

where T—air temperature at 2 m height (°C), u_2—wind speed at 2 m height (ms^{-1}), e_s—saturation vapour pressure (kPa), e_a—actual vapour pressure (kPa), ($e_s - e_a$)—saturation vapour deficit (kPa), R_n—net radiation at the crop surface ($MJm^{-2}\ day^{-1}$), G—soil heat flux density ($MJm^{-2}\ day^{-1}$), Δ—slope vapour pressure curve (kPa $°C^{-1}$), γ—psychrometric constant (kPa $°C^{-1}$).

The above equation determines the evapotranspiration (ET_o) from the hypothetical grass reference surface. The effect of soil heat flux (G) is ignored for daily calculations [6] as the magnitude of the heat flux in this case is relatively small. The FAO Penman-Monteith method [6] is still used as the sole standard method as could be seen in recent research work on reference evapotranspiration included in [26, 27], etc. However, since the number of requested climatic variables is often not available under limited data conditions [28, 29], other simple ETo equations with less number of requested climatic variables have been used to compute ETo values that are close to the FAO Penman-Monteith method. These methods are the four of the Valiantzas equations, along with the Makkink, Calibrated Hargreaves, Abtew, Jensen-Haise, and Caprio equations and could be used as best alternative ET_o estimation methods. These alternative equations could be used across the dry semi-arid and arid zones where water is the most limiting factor to food and fiber production [27].

The maize crop variety used in this study is the 118-day one whose phenology is as follows: 20 days for initial, 32 days for development, 38 days for mid-season, and 28 days for late season growth stages. This is based on the what is stated in [6] that the length of crop development stages provided in their table is indicative of general conditions; the user is therefore strongly encouraged to obtain appropriate local information.

2.3.3 Dry day and critical dry spell definition

It is usual to use rainfall thresholds higher than zero millimeter to define a dry day in order to account for the measurement errors or very little amounts of rain that are not available for plants or water resources, due to interception and/or direct evaporation [29, 30]. Different precipitation thresholds of 1–10 mm/day but fixed for the whole observation period are considered by most authors in analyzing long dry spells [30–33]. However, since the evaporation varies throughout the year and for different locations, fixed rainfall thresholds are not representative of real ground conditions. The net precipitation that is available for plants can be strongly modulated by atmospheric evaporative demands thereby affecting water stress levels by plants and crops [34–36]. Meteorological data from different approaches such as potential evaporation [37] or the reference evapotranspiration [6] can be used to determine atmospheric evaporative demand. Rivoire et al. [38] emphasized the need to take account of the atmospheric evaporative demand instead of making use of fixed rainfall thresholds for defining a dry day when analyzing dry spells with respect to agricultural impacts in particular. A dry day in this work is therefore taken as the day when the rainfall (RR) is less than the average reference evapotranspiration, ET_o [38, 39]. A threshold of ET_o is considered to define a dry day when $RR–ETo \leqq 0$ [38]. A number of these consecutive dry days constitute a spell. The critical dry spells are therefore those that occur at germination/emergence and establishment (initial stage), and close to and during the tasseling and flowering stage (mid-season stage). However, the critical dry spell prediction carried out in this work is for the mid-season stage only. **Figure 1** shows the time series of rainfall and mean reference evapotranspiration against day of the year from around planting date to harvesting date for maize crop for 1973 in Ibadan. Four critical dry spells during the mid-season are indicated. The minimum number of consecutive dry days that constitute a spell in this work is 3 days [40].

2.3.4 Artificial neural network (ANN) model

2.3.4.1 Model description

Artificial neural network (ANN) model was used in this work for the prediction of mid-growing season critical dry spell onset dates and lengths. ANN is a "black box" model of a type that is often used to model high-dimensional nonlinear data. It is a nonstatistical data modeling tool, which is contained in any version of R statistic or Matlab tool box. ANN is a highly interconnected network of machine learning algorithm based on the model of a human neuron. It mimics this model or structure by distributing its computations to small and simple processing units called artificial neurons or nodes [41, 42]. Artificial intelligence (AI) makes it possible for machines to learn from experience, adjust to new inputs, and perform human-like tasks. According to [42], ANN is data-driven, self-adaptive methods since there are few known assumptions about the models for problems under study unlike the traditional model-based methods. ANN model learns from examples and captures subtle functional relationships among the data even if the underlying relationships are unknown or hard to describe. This makes ANN very appropriate for problems whose solutions require knowledge that is not easy to state explicitly but for which there are enough observations [42]. Therefore, they can be treated as one of the multivariate nonlinear nonparametric statistical methods [43, 44]. After learning the data presented to them, ANN can generalize and often correctly infer the unseen part of a population even if the sample data contain noisy information. Since ANNs can compute the value of any continuous function to any desired accuracy as has been shown by [45–47], they are considered as universal functional approximators [42].

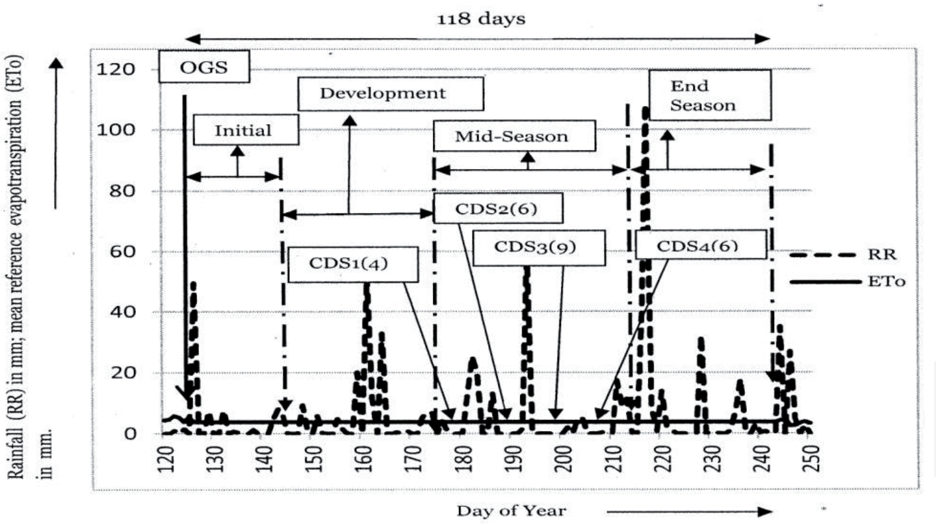

Figure 1.
Time series of rainfall (RR in mm) and mean reference evapotranspiration (ETo in mm) from the onset date of growing season, OGS (in days of year) for 118-day maize crop to its harvesting time for 1973 in Ibadan. $CDS_1(4)$, $CDS_2(6)$, $CDS_3(9)$, and $CDS_4(6)$ represent the first, second, third, and fourth critical dry spells with lengths 4, 6, 9, and 6 days in brackets, respectively. Mean (1971–2013) reference evapotranspiration for growing season for maize is approximately 3.72 mm.

ANN is made up of three layers of units, the input, hidden, and output layers. The ANN receives the input signal from the external world in the form of a pattern and image in the form of a vector. Each of the input is then multiplied by its corresponding weights. These weights are the details used by the ANNs to solve a certain problem. The activity of the input layer represents the raw information that is fed into the network, while the activities of each hidden layer are determined by the activities of the input layer and the weights on the connections between the input and the hidden layer. The behavior of the output layer depends on the activity of the hidden layer and the weights between the hidden and the output layers. To train the neural network models, the training parameters for the chosen algorithm must be specified in terms of the inputs, the number of hidden and output layer neurons, and the activation function of each layer [41, 48]. To fulfill these requirements, the correct number of regressor as well as the number of hidden neurons must first be selected but there are no specific rules for these selections [49, 50]. In many applications, the number of neurons for the hidden layer is selected based on trial-and-error method usually starting with small initial network [51]. A sample ANN architecture for first critical dry spell onset date prediction for Ibadan is shown in **Figure 2** having one input layer of nine neurons, two hidden layers—first of nine neurons and second of two neurons—and one output layer of one neuron. The inputs are multiplied by modifiable weights that are crucial parameters of the ANN models for solving a problem. ANN model could be run in R software—in R studio [52]. The neuralnet package (neuralnet) version 1.33 of August 5, 2016 [53] was used in this work. The training of neural networks uses the back-propagation, resilient back-propagation with [54] or without weight backtracking [55], or the modified globally convergent version by [56]. The package allows flexible settings through custom choice of error and activation function and it can combine fast convergence and stability and generally provides good results [55]. Furthermore, the calculation of generalized weights [58] is implemented. In this work, the default neural algorithm was used (i.e., "rprop+"). This refers to the resilient back-propagation with weight backtracking [54]. Amid the pool of the weight-updating process, the resilient back-propagation (RProp algorithm from the "nuerlanet" package in R) was chosen because it can combine fast convergence and stability and generally provides good results.

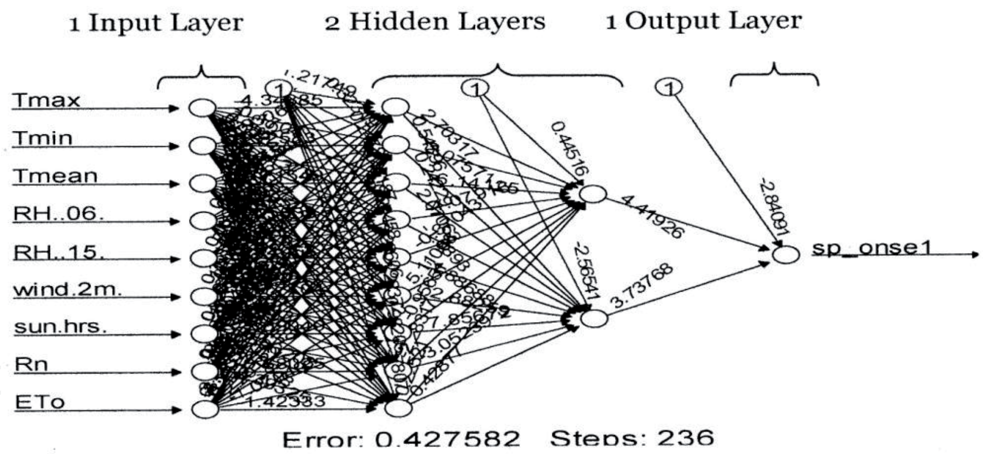

Figure 2.
A sample ANN architecture for first critical dry spell onset date prediction for 2008 for Ibadan, Nigeria.

2.3.4.2 Prediction procedure

The data attributes (predictors) used in the neural network model were maximum, minimum, and mean temperatures (T_{max}), (T_{min}), and (T_{mean}), relative humidity at 0600 (RH_{06}) and 1500 (RH_{15}) GMT, wind speed at 2 m level (u_2), sunshine hours (n), net radiation (R_n), and reference evapotranspiration (ET_o), while the data classes (predictands) were onset dates and lengths of critical dry spells. Net radiation and reference evapotranspiration were computed. In this work, the 43-year data were partitioned into two: 30 years for training and 13 independent years for testing. The test data were kept out of the process of producing the ANN model in order to test its predictive power [14]. This corresponds to approximately 70% (two-thirds) of data for training and 30% (one-third) for testing. Regarding the data partitioning, some authors have used two-thirds of data for training and one-third for validation and testing [57–59]. Dubey [58] used approximately half of one-third of data each for validation and testing. However, Mulualem and Liou [14] who worked on the application of artificial neural networks in forecasting a standardized precipitation evaporative index (SPEI) for the Upper Blue Nile Basin, Ethiopia (using RProp algorithm from the “neuralnet” package in R), partitioned their data into training and test sets. This method was applied in this work. The two independent datasets were chosen in such a way that early, normal, and late onset dates of critical dry spells were reflected in each of them. Likewise, the lowest, normal, and highest lengths of critical dry spells were also reflected in each of them. The neural network architecture consists of one input layer, one or two hidden layers, and one output layer. The input layer (first layer) of neurons consists of the nine attributes (predictors). The hidden layers of neurons are two (the second and third layers) and in few cases one. The hidden layer neurons are generally chosen starting with lower number neurons and varying by trial and error till the configuration that gives minimum root-mean-square error is attained. The output (third or fourth layer) layer consists of one neuron of either onset date or length of critical dry spell. Two hidden layer networks may provide more benefits for some type of problems [60]. Several authors addressed this problem and considered more than one hidden layer (usually two hidden layers) in their network design processes.

A cross-correlation analysis was performed to measure the relationship between the predictors (attributes) and the predictands (classes). Positive and negative relationships were observed, some with weak relationships. Based on the cross-correlations, seven different ANN models shown in **Table 2** below are put forward for each station with a view to measuring their predictive ability by

Model	No. of input variable	Max. Temp	Min. Temp	Mean Temp	R. H. (06 GMT)	R. H. (15 GMT)	Wind Speed (2 m)	Sun hr.	Net Rad. (Rn)	Ref. evap. (ETo)
M1	9	✓	✓	✓	✓	✓	✓	✓	✓	✓
M2	8	✓	✓	✓	✓	—	✓	✓	✓	✓
M3	7	✓	✓	✓	✓	✓	✓	—	✓	—
M4	6	✓	✓	—	✓	—	✓	—	✓	✓
M5	5	✓	✓	—	✓	—	✓	—	✓	—
M6	4	✓	✓	—	—	—	✓	—	✓	—
M7	3	✓	—	—	—	—	✓	—	✓	—

Table 2.
Input variables used in the attempt to get suitable models (M1–M7) for the prediction of onset dates and lengths of critical dry spells.

comparing predicted values with the observed ones. A measure of ANN most suitable model performance on the basis of all statistical measures of the observed and predicted critical dry spell onset dates and lengths for the nine stations are shown in **Tables 3** and **4**. Out of the seven models used with these predictors, Model 1 having nine parameters was noted to be quite suitable for most of the stations, while models 2, 3, and 5 having eight, seven, and five parameters respectively were more suitable than Model 1 in some cases. Predictions (testings) were made for two regular mid-growing season critical dry spells (first and second) for all stations. Predictions were made on yearly basis on the twentieth (20th) day after the onset

Sta. name	Most suitable model (M) for dry spell onset	Neural net. Arch.	Lead time pred. Range (days)	RMSE	R^2	NSE	WIA	RSR	Prediction error margin (days)
Cal	M1-On Date1	9–3-1	27–34	1.53	0.75	0.72	0.89	0.50	−3.09 to 3.22
	M1-On Date2	9–9-1	41–56	2.93	0.82	0.82	0.95	0.40	−4.56 to 4.89
War	M1-On Date1	9–8–2-1	31–43	2.95	0.86	0.77	0.92	0.47	−4.67 to 3.01
	M1-On Date2	9–9–2-1	43–66	3.31	0.83	0.80	0.95	0.42	−1.08 to 4.75
Iba	M3-On Date1	7–9–2-1	15–26	1.42	0.80	0.64	0.93	0.57	−1.46 to 1.91
	M2-On Date2	8–9–9-1	28–37	2.07	0.70	0.65	0.90	0.56	−3.45 to 2.64
Ilo	M1-On Date1	9–8–1-1	17–24	1.65	0.70	0.68	0.91	0.53	−3.18 to 2.23
	M1-On Date2	9–8–1-1	30–37	1.54	0.86	0.85	0.96	0.37	−2.69 to 3.23
Lok	M1-On Date1	9–8–6-1	13–32	2.19	0.79	0.79	0.94	0.44	−3.07 to 3.89
	M5-On Date2	5–2-1	28–36	2.05	0.58	0.48	0.88	0.69	−3.55 to 3.15
Mak	M1-On Date1	9–9–8-1	20–24	1.12	0.75	0.59	0.82	0.61	−1.47 to 2.04
	M1-On Date2	9–8–4-1	26–44	2.70	0.79	0.76	0.94	0.46	−3.64 to 4.02
Yel	M1-On Date1	9–8–7-1	18–22	2.40	0.71	0.66	0.91	0.55	−4.04 to 3.42
	M1-On Date2	9–3-1	28–41	3.07	0.72	0.72	0.91	0.50	−4.29 to 4.07
Kad	M1-On Date1	9–9–2-1	13–28	2.67	0.71	0.65	0.91	0.56	−3.85 to 3.11
	M2-On Date2	8–7–1-1	26–34	2.37	0.79	0.74	0.93	0.48	−4.24 to 3.24
Yol	M1-On Date1	9–7–1-1	13–25	3.16	0.67	0.57	0.90	0.62	−3.40 to 2.63
	M1-On Date2	9–8–8-1	23–35	2.46	0.73	0.64	0.90	0.57	−4.08 to 4.24

Table 3.
A measure of ANN most suitable model performance on the basis of all statistical measures of the observed and predicted critical dry spell onset dates for the nine stations.

Agro-eco. zones	Sta. name	Most suitable model (M) for dry spell length	Neural net. arch.	RMSE	R^2	NSE	WIA	RSR	Prediction error margin (days)
Mangrove Swamp	Cal	M1-Len1	9–2–1	0.74	0.81	0.77	0.94	0.45	−0.97 to 1.27
		M5-Len2	5–3–1	0.97	0.69	0.67	0.87	0.55	−1.43 to 1.30
	War	M3-Len1	7–3–1	0.93	0.85	0.82	0.94	0.40	−1.32 to 1.51
		M1-Len2	9–5–4–1	0.46	0.92	0.69	0.94	0.53	−0.01 to 1.00
Rain Forest	Iba	M1-Len1	9–9–1–1	1.49	0.78	0.57	0.86	0.65	−1.71 to 2.02
		M1-Len2	9–4–1	1.52	0.75	0.57	0.79	0.62	−2.76 to 2.01
Southern Guinea Savannah	Ilo	M1-Len1	9–4–1	2.05	0.68	0.51	0.84	0.66	−3.38 to 2.68
		M2-Len2	8–4–1	0.79	0.93	0.90	0.98	0.30	−2.05 to 1.19
	Lok	M1-Len1	9–2–1	1.72	0.78	0.58	0.83	0.61	−1.45 to 2.91
		M1-Len2	9–2–1	1.61	0.82	0.55	0.87	0.64	−0.84 to 2.90
	Mak	M1-Len1	9–5–2–1	1.83	0.63	0.55	0.86	0.63	−2.27 to 2.41
		M1-Len2	9–5–4–1	1.83	0.71	0.63	0.91	0.58	−3.51 to 3.22
Northern Guinea Savannah	Yel	M1-Len1	9–8–1–1	1.71	0.78	0.64	0.89	0.59	−2.71 to 3.24
		M1-Len2	9–3–1	0.90	0.67	0.66	0.89	0.55	−1.33 to 1.51
	Kad	M1-Len1	9–3–1	1.85	0.76	0.58	0.83	0.61	−3.72 to 1.03
		M1-Len2	9–3–1	0.68	0.89	0.83	0.94	0.39	−1.34 to 0.91
	Yol	M1-Len1	9–3–1	1.65	0.71	0.67	0.87	0.55	−3.47 to 2.48
		M5-Len2	5–2–1–1	0.93	0.75	0.62	0.87	0.59	−0.93 to 1.93

***Cal, War, Iba, Ilo, Lok, Mak, Yel, Kad, Yol**—Calabar, Warri, Ibadan, Ilorin, Lokoja, Makurdi, Yelwa, Kaduna, Yola; **M1 .. M7**—Model1 .. Model7; **On Date1, On Date2**—First Onset Date, Second Onset Date; **Len1, Len2**—First Spell Length, Second Spell Length; **RMSE**—Root-Mean-Square Error; **R2**—Coefficient of Determination;* **NSE**—*Nash-Sutcliffe Coefficient of Efficiency;* ***WIA**—Wilmott's Index of Agreement; **RSR**—RMSE-Observations Standard Deviation Ratio.*

Table 4.
A measure of ANN most suitable model performance on the basis of all statistical measures of the observed and predicted critical dry spell lengths for the nine stations.

dates of growing season for Calabar and Warri with use of 10-day average values of the attributes (predictors), that is, average taken from the eleventh (11th) day through twentieth (20th) day. However, for the remaining seven stations, yearly predictions were made for the first and second critical dry spell onset dates and lengths on the thirtieth (30th) day after the onset dates of growing season with the use of 10-day average values of the attributes (predictors), that is, average taken from the twenty-first (21st) day through the thirtieth (30th) day. The choice of the 10-day average of the predictors and the choice of the beginning date were basically by trial and error until good predictors were realized. The predictions made for the onset dates of critical dry spells were actually for the number of days before the occurrence of first and second critical dry spells from the 20th or 30th day after the onset dates of growing season. So, the onset dates of the critical dry spells in terms of days of the year should be onset dates of growing season (in days of the year) plus 20 days (for Calabar and Warri) or 30 days (for the remaining seven stations) plus the number of days before the occurrence of the critical dry spell. These are indicated in Eqs. (2) and (3) respectively below:

For Calabar and Warri Stations (two station):

$$\mathrm{CDS_{OD}}\ (\text{day of year}) = \mathrm{OGS}\ (\text{day of year}) + 20 + \mathrm{NoD} \tag{2}$$

For Ibadan, Ilorin, Lokoja, Makurdi, Yelwa, Kaduna, and Yola Stations (seven stations):

$$CDS_{OD}\text{ (day of year)} = OGS\text{ (day of year)} + 30 + NoD \tag{3}$$

where CDS_{OD} (day of year)—Critical Dry Spell Onset Date in days of year, OGS (day of year)—Onset Date of Growing Season in days of year, and NoD—number of days before the occurrence of the critical dry spell.

For any year, the normalized attributes (predictors) were substituted in the prediction equations (not shown) derived from the neural network architecture involving the input (predictors), hidden, and output (predictands) neurons. Normalized values of the predictors were used in the equation to limit the output to a range between 0 and 1, making the function useful in the prediction of probabilities. Outputs of hidden layer neurons and output layer neuron were determined using Sigmoid Activation Function. The purpose of the sigmoid activation function is to introduce nonlinearity into the output of a neuron. Neural network has neurons that work in correspondence of weight, bias, and activation function. After prediction, the predicted values were converted to actual values by the removal of the normalization.

3. Results and discussions

3.1 Warri and Calabar

Figure 3(a) and **(b)** gives the *first and second* respectively yearly actual and predicted values of mid-season critical dry spell onset dates and lengths for Warri in the Mangrove Swamp agro-ecological zone. The actual and predicted values of the onset dates of first and second critical dry spells are actually the *number of days* before the occurrence of the critical dry spells *from 20th day* after the onset dates of growing season. So, the predicted onset dates of the critical dry spells in terms of days of the year should be onset dates of growing season (in days of the year) plus 20 days plus the predicted number of days before the occurrence of the critical dry spell (Eq. (2)). The prediction lead times for first and second critical dry spell onset dates range from 31 to 66 days for Warri and from 27 to 56 days for Calabar (figure not shown) as shown in **Table 3**. The range of errors during testing for onset dates and lengths for the first and second critical dry spells is generally ±4 days for Warri and for Calabar (figure not shown). The root-mean-square errors (RMSE), coefficient of determination (R^2), Nash-Sutcliffe Coefficient of Efficiency (NSE), Wilmott's Index of Agreement (WIA), and RMSE-Observations Standard Deviation Ratio (RSR) for first and second critical dry spell *onset dates* for Warri range from 2.95 to 3.31, 0.83 to 0.86, 0.77 to 0.80, 0.92 to 0.95, and 0.42 to 0.47 days, respectively, while those for Calabar (figure not shown) range from 1.53 to 2.93, 0.75 to 0.82, 0.72 to 0.82, 0.89 to 0.95, and 0.40 to 0.50 days, respectively (**Table 3**). The RMSE, R^2, NSE, WIA, and RSR for the first and second critical dry spell *lengths* for Warri range from 0.46 to 0.93, 0.85 to 0.92, 0.69 to 0.82, 0.94 to 0.94, and 0.40 to 0.53 days, respectively, while those for Calabar (figure not shown) range from 0.74 to 0.97, 0.69 to 0.81, 0.67 to 0.77, 0.87 to 0.94, and 0.45 to 0.55 days, respectively (**Table 4**). The neural network architecture for the first and second onset dates and lengths of the critical dry spells for both stations are given in **Tables 3** and **4**.

Ogunrinde et al. [3] who applied ANN for forecasting Standardized Precipitation and Evapotranspiration Index (SPEI): A case study of Nigeria got an RMSE value of 0.7476 for Ikeja, a station in Lagos State, Western Nigeria in the same agro-ecological

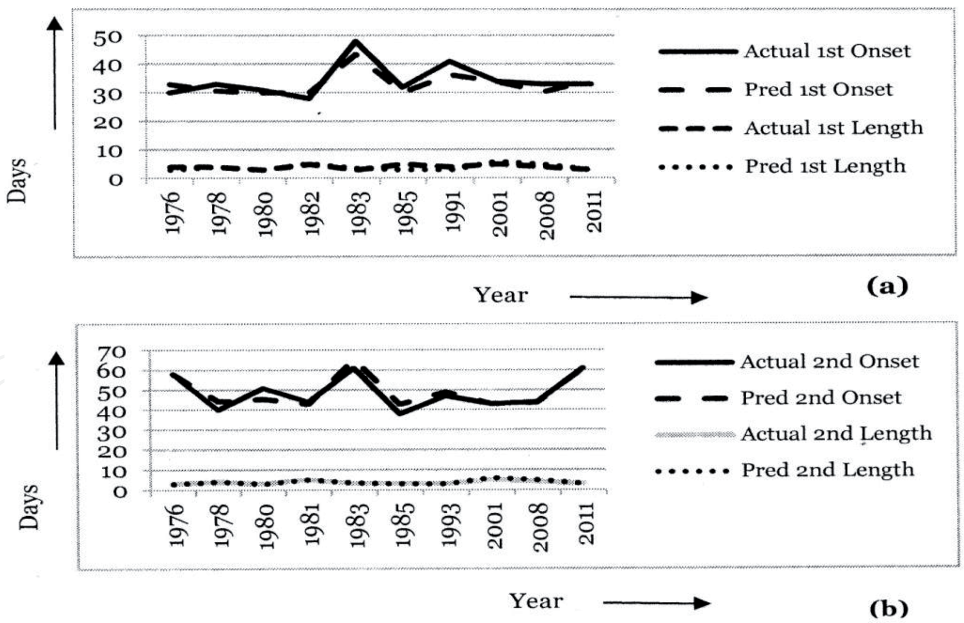

Figure 3.
Yearly prediction of (a) mid-season first critical dry spell onset dates and lengths (b) mid-season second critical dry spell onset dates and lengths in Warri. The critical dry spell onset dates are given in terms of the number of days before the critical dry spell occurrence from the 20th day after the onset dates of growing season.

zone with Warri and Calabar. The two values are somehow close especially for the initial aspect of the range for the critical dry spell lengths even though the forecasts in the current work are for the onset dates and lengths of mid-season critical dry spells and not for SPEI. Dry spell onset dates and lengths prediction were not carried out by these and other researchers. So, on the 20th day after the onset date of growing season of any year in Warri and Calabar, maize farmers could be given yearly advance information on the dates of occurrence of first and second critical dry spells and their respective lengths for the mid-season (tasseling and flowering of maize). This would enable them make adequate preparations for their farming operations to ensure improved maize yield taking cognizance of the error margins.

3.2 Ibadan

The yearly actual and predicted values of the *first and second* mid-season critical dry spell onset dates and lengths are shown in **Figure 4(a)** and **(b)** respectively for Ibadan in the Rain Forest agro-ecological zone. The actual and predicted values of the onset dates of first and second critical dry spells are actually the *number of days* before the occurrence of the critical dry spells *from 30th day* after the onset dates of growing season. So, the actual and predicted onset dates of the critical dry spells in terms of days of the year should be onset dates of growing season (in days of the year) plus 30 days plus the predicted number of days before the occurrence of the critical dry spell (Eq. (3)). The first and second critical dry spell onset date prediction lead times range from 15 to 37 days in Ibadan (**Table 3**). The range of errors during testing for onset dates and lengths for the first and second critical dry spells is generally ±4 days. The RMSE, R^2, NSE, WIA, and RSR for first and second critical dry spell *onset dates* for Ibadan range from 1.42 to 2.07, 0.70 to 0.80, 0.64 to 0.65, 0.90 to 0.93, and 0.56 to 0.57 days, respectively (**Table 3**), while those for first and second critical dry spell *lengths* range from 1.49 to 1.52, 0.75 to 0.78, 0.57 to 0.57, 0.79 to 0.86, and 0.62 to 0.65 days, respectively (**Table 4**). The neural network architecture for first and second onset dates and lengths of the critical dry spells for Ibadan are also given in **Tables 3** and **4**.

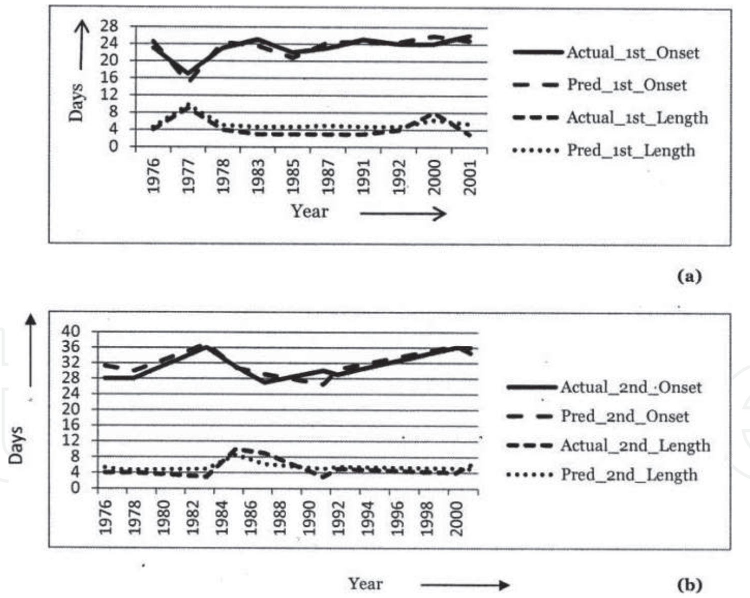

Figure 4.
Yearly prediction of (a) mid-season first critical dry spell onset dates and lengths (b) mid-season second critical dry spell onset dates and lengths in Ibadan. The critical dry spell onset dates are given in terms of the number of days before the critical dry spell occurrence from the 30th day after the onset dates of growing season.

The result of the work of Morid et al. [15] regarding ANN forecast of Effective Drought Index (EDI) (6 months in advance) in Mehrabad station using nine input models gave validation RMSE values ranging from 0.55 to 1.51. Though the latitudes of Ibadan and Mehrabad differ and the target forecasts also differ, the range of RMSE values is somewhat close. The predictions of critical dry spell onset dates and lengths were not addressed by the researchers.

Therefore, on the 30th day after the onset date of growing season of any year in the station, maize farmers could be given advance information on the dates of occurrence of first and second critical dry spells and their respective lengths to enable them make informed preparations in their farming operations for enhanced maize yield taking note of the error margins.

3.3 Makurdi, Ilorin, and Lokoja

Figure 5(a) and **(b)** shows the *first* and *second* respectively yearly actual and predicted values of mid-season critical dry spell onset dates and lengths for Makurdi in the Southern Guinea Savannah agro-ecological zone. The actual and predicted values of the onset dates of first and second critical dry spells are actually the *number of days* before the occurrence of the critical dry spells *from 30th day* after the onset dates of growing season. So, the predicted onset dates of the critical dry spells in terms of days of the year should be onset dates of growing season (in days of the year) plus 30 days plus the predicted number of days before the occurrence of the critical dry spell (Eq. (3)). The first and second critical dry spell onset date prediction lead times range from 20 to 44 days for Makurdi, those for Ilorin (figure not shown) range from 17 to 37 days, while those for Lokoja (figure not shown) range from 13 to 36 (**Table 3**). The range of errors during testing for onset dates and lengths of the first and second critical dry spells is generally ±4 days for each of the stations—Makurdi, Ilorin (figure not shown), and Lokoja (figure not shown). The RMSE, R^2, NSE, WIA, and RSR for first and second critical dry spell *onset dates* for Makurdi range from 1.12 to 2.70, 0.75 to 0.79, 0.59 to 0.76, 0.82 to 0.94, and 0.46 to 0.61 days, respectively, those for Ilorin (figure not shown) range from 1.54 to 1.65, 0.70 to 0.86, 0.68 to 0.85, 0.91 to 0.96 and 0.37 to 0.53 days,

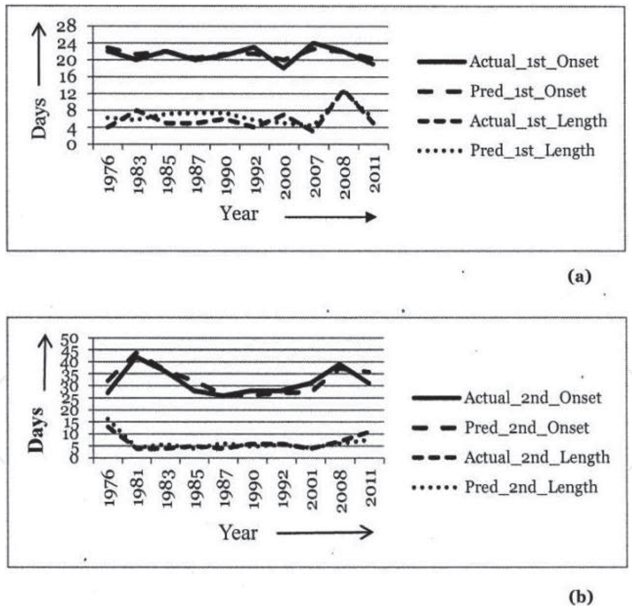

Figure 5.
Yearly prediction of (a) mid-season first critical dry spell onset dates and lengths (b) mid-season second critical dry spell onset dates and lengths respectively in Makurdi. The critical dry spell onset dates are given in terms of the number of days before the critical dry spell occurrence from the 30th day after the onset dates of growing season.

respectively, while those for Lokoja (figure not shown) range from 2.05 to 2.19, 0.58 to 0.79, 0.48 to 0.79, 0.88 to 0.94, and 0.44 to 0.69 days, respectively(**Table 3**). The RMSE, R^2, NSE, WIA, and RSR for first and second critical dry spell *lengths* for Makurdi range from 1.83 to 1.83, 0.63 to 0.71, 0.55 to 0.63, 0.86 to 0.91, and 0.58 to 0.63 days, respectively; those for Ilorin (figure not shown) range from 0.79 to 2.05, 0.68 to 0.93, 0.51 to 0.90, 0.84 to 0.98, and 0.30 to 0.66 days, respectively, while those for Lokoja (figure not shown) range from 1.61 to 1.72, 0.78 to 0.82, 0.55 to 0.58, 0.83 to 0.87, and 0.61 to 0.64 days, respectively (**Table 4**). The neural network architecture for first and second onset dates and lengths of the critical dry spells for the three stations are given in **Tables 3** and **4**.

Ogunrinde et al. [3] in their work on ANN for forecasting SPEI: A case study of Nigeria (for drought matters) got an RMSE value of 0.5957 for Lokoja station. The difference in the values got for critical dry spell length in the present work is possibly as a result of different target forecasts—SPEI as distinct from mid-season critical dry spell lengths. Therefore, on the 30th day after the onset date of growing season of any year in the stations, maize farmers could be given yearly advance information on the dates of occurrence of first and second critical dry spells and their respective lengths. This would enable farmers make necessary plans for their farming operations for enhanced maize yield noting the prediction error margins.

3.4 Kaduna, Yelwa, and Yola

The yearly actual and predicted values of *first* and *second* mid-season critical dry spell onset dates and lengths are presented in **Figure 6(a)** and **(b)** respectively for Kaduna in Northern Guinea Savannah agro-ecological zone. The actual and predicted values of the onset dates of first and second critical dry spells are actually the *number of days* before the occurrence of the critical dry spells *from 30th day* after the onset dates of growing season. So, the predicted onset dates of the critical dry spells in terms of days of the year should be onset dates of growing season (in days of the year) plus 30 days plus the predicted number of days before the occurrence of the critical dry spell (Eq. (3)). The prediction lead times for first and second

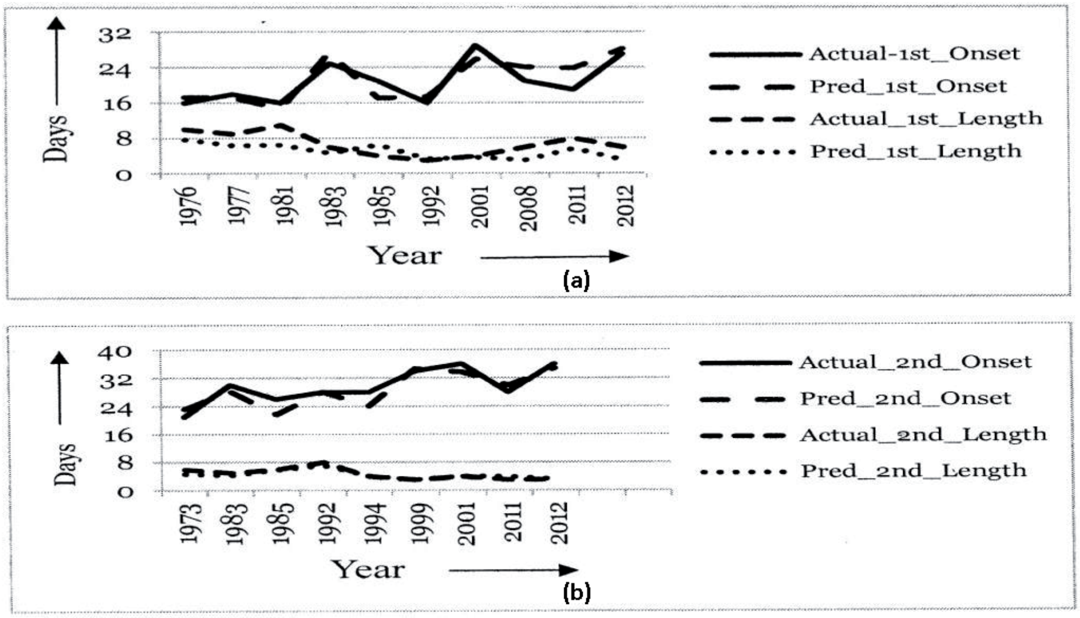

Figure 6.
Yearly prediction of (a) mid-season first critical dry spell onset dates and lengths (b) mid-season second critical dry spell onset dates and lengths respectively in Kaduna. The critical dry spell onset dates are given in terms of the number of days before the critical dry spell occurrence from the 30th day after the onset dates of growing season.

critical dry spells range from 13 to 34 days for Kaduna. Those for Yelwa (figure not shown) range from 18 to 41 days, while those for Yola (figure not shown) range from 13 to 35 days (**Table 3**). The range of errors during testing for onset dates and lengths of the first and second critical dry spells is generally ±4 days for each of the stations—Kaduna, Yelwa (figure not shown), and Yola (figure also not shown). The RMSE, R^2, NSE, WIA, and RSR for *onset dates* of first and second critical dry spells for Kaduna range from 2.37 to 2.67, 0.71 to 0.79, 0.65 to 0.74, 0.91 to 0.93, and 0.48 to 0.56 days, respectively. Those for Yelwa (figure not shown) range from 2.40 to 3.07, 0.71 to 0.72, 0.66 to 0.72, 0.91 to 0.91, and 0.50 to 0.55 days, respectively, while those for Yola (figure not shown) range from 2.46 to 3.16, 0.67 to 0.73, 0.57 to 0.64, 0.90 to 0.90, and 0.57 to 0.62 days, respectively (**Table 3**). The RMSE, R^2, NSE, WIA, and RSR for first and second critical dry spell *lengths* for Kaduna range from 0.68 to 1.85, 0.76 to 0.89, 0.58 to 0.83, 0.83 to 0.94, and 0.39 to 0.61 days, respectively, those for Yelwa (figure not shown) range from 0.90 to 1.71, 0.67 to 0.78, 0.64 to 0.66, 0.89 to 0.89, and 0.55 to 0.59 days, respectively, while those for Yola (figure not shown) range from 0.93 to 1.65, 0.71 to 0.75, 0.62 to 0.67, 0.87 to 0.87, and 0.55 to 0.59 days, respectively (**Table 4**). The neural network architecture for the first and second onset dates and lengths of the critical dry spells for the three stations are also given in **Tables 3** and **4**.

Mulualem and Liou [14] in their work on ANN in forecasting SPEI for the Upper Blue Nile Basin in Ethiopia got RMSE value of 0.428 for Bahdir Dar of almost the same latitude with Yelwa, Nigeria. The value of 0.91–1.71 got for critical dry spell length got in the current work is somehow close. However, the difference in the values could be as a result of different target forecasts—SPEI as distinct from mid-season critical dry spell lengths. Therefore, on the 30th day after the onset date of growing season of any year in the stations, maize farmers could be given advance information on the dates of occurrence of first and second critical dry spells and their respective lengths to enable them make adequate plans for their farming operations for improved maize yield. The prediction could be made using ANN on 30th day after growing season onset dates for these critical dry spells with 10-day average values of the predictors (attributes) taken from 21st to 30th day with minimum lead times of about 2 weeks and maximum of about 2 month as given above (**Table 3**). To make predictions for any year, the predictors (attributes) are first normalized and substituted into the equation (not shown) derived from the neural network architecture involving the input, hidden and output layers, weights, and sigmoid activation functions. At the result stage, the normalization is removed to get the actual onset dates and lengths of the critical dry spells—predictands (classes).

4. Conclusions and recommendation

The prediction of mid-season critical dry spell onset dates and lengths for 118 day rain-fed maize crop in Nigeria using ANN has yielded the following useful results that include the following: (a) the provision of yearly advance information on the number of days before the occurrence of first and second critical dry spells and their respective lengths on 20th day after the onset dates of growing season in Calabar and Warri; (b) the provision of yearly advance information on the number of days before the occurrence of first and second critical dry spell onset dates and lengths on 30th day after the onset dates of growing season in Ibadan, Ilorin, Lokoja, Makurdi, Yelwa, Kaduna, and Yola in Nigeria. The minimum prediction lead time is about 2 weeks, while the maximum is about 2 months. This information will aid yearly supplementary irrigation planning, scheduling, and various other decision makings related to sustainable agricultural operations for enhanced 118-day maize yield in the nine stations in Nigeria. For future work, it is recommended that more stations and longer years of data be used to ensure adequate training of ANN networks to realize better prediction results and gain more insight into dry spell occurrences during mid-growing seasons in Nigeria.

Acknowledgements

We are grateful to Dr. Imoleayo Gbode for his technical assistance regarding the downloads and use of neuralnet package for this work. We are indebted to the former Director General/Chief Executive Officer of Nigerian Meteorological Agency (NiMet) and Dr. A. C. Anuforom, for the provision of the data used for this work. We thank immensely the former Director of West African Science Center for Climate Change and Adapted Land Use (WASCAL) of The Federal University of Technology, Akure, Nigeria, Prof. K. O. Ogunjobi, for granting permission for the use of its Internet facility. We place on record the technical assistance of Dr. O. Adeyeri on matters of data homogenization. The Director of the Centre for Continuing Education, The Federal University of Technology, Akure, Prof. E. C. Okogbue is highly appreciated for his good advice in this work and for the provision of some academic facility used for this work.

Conflict of interest

The authors declare that they have no conflict of interest as regards the publication of this article.

Author details

Nnadozie Okonkwo Nnoli[1]*, Ahmed Balogun[1], Jerome Omotosho[1] and Samuel Agele[2]

1 Department of Meteorology and Climate Science, The Federal University of Technology, Akure, Nigeria

2 Department of Crop, Soil and Pest Management, The Federal University of Technology, Akure, Nigeria

*Address all correspondence to: nnolino@futa.edu.ng; nonnoli48@gmail.com

References

[1] Song Y, Tian J, Linderholm HW, Wang C, Ou Z, Chen D. The contributions of climate change and production area expansion to drought risk for maize in China over the last four decades. International Journal of Climatology. 2020;41(sup 1): E2851-E2862. DOI: 10.1002/joc.6885

[2] Yu X, He X, Zheng H, et al. (2013) Spatial and temporal analysis of drought risk during the crop-growing season over Northeast China. NatHazards. 2013;**71**:275-289

[3] Ogunrinde AT, Oguntunde PG, Fasinmirin JT, Akinwumiju AS. Application of artificial neural network for forecasting standardized precipitation and evapo-transpiration index: A case study of Nigeria. Engineering Reports. 2020;**2020**:e12194. DOI: 10.1002/eng2.12194 wileyonlinelibrary.com/journal/eng2

[4] Mugalavai EM, Kipkorir EC, Songok CK. Evaluation of dry spells during sensitive growth stages for maize crop in Western Kenya. In: The International Conference on Disaster Risk Reduction and Conflict Resolution for Sustainable Development 18-20th July, 2012. Kakamega, Kenya: @ Mmust; 2012

[5] Gao C, Li X, Sun Y, et al. 2019 Water requirement of summer maize at different growth stages and the spatiotemporal characteristics of agricultural drought in the Huaihe River Basin, China. Theoretical and Applied Climatology. 2019;**136**:1289-1302. DOI: 10.1007/s00704-018-2558-6

[6] Allen RG, Pereira LS, Raes D, Smith M. FAO Crop Evapotranspiration - Guidelines for Computing Crop Water Requirements; FAO Irrigation and Drainage Paper 56. Rome, Italy; 1998:1-300

[7] Sharma TC. Challenges in drought research: Some perspectives and future directions. Hydrological Science Journal. 2002;**47**(sup 1):S19-S30. DOI: 10.1080/02626660209493019

[8] IPCC. Special Report on Managing the Risk of Extreme Events and Disasters to Advance Climate Change Adaptation. Cambridge, UK: Cambridge University Press; 2012. p. 582

[9] Wilhite DA, Sivakumar MVK, Pulwarty R. Managing drought in a changing climate: The role of national drought policy weather and climate. Extremes. 2014;**3**(2014):4-13

[10] Box GEP, Jenkins GM. Time Series Analysis: Forecasting and Control. San Francisco, Calif, USA: Holden-Day; 1976

[11] Gbangou T, Ludwig F, van Slobbe E, Greuell W, Kranjac-Berisavljevic G. Rainfall and dry spell occurrence in Ghana: Trends and seasonal predictions with a dynamical and a statistical model. Theoretical and Applied Climatology. 2020;141:371-387. DOI: 10.1007/s00704-020-03212-5

[12] Mishra SS, Nagarajan R. Forecasting drought in Tel River Basin using feed-forward recursive neural network. In: 2012 International Conference on Environmental, Biomedical and Biotechnology IPCBEE vol. 41 (2012) © (2012). Singapore: IACSIT Press; 2012

[13] Abrishami N, Sepaskhah AR, Shahrokhnia MH. Estimating wheat and maize daily evapotranspiration using artificial neural network. Theoretical and Applied Climatology 2019;135: 945-958. https://doi.org/10.1007/s00704-018-2418-4

[14] Mulualem GM, Liou Y-A. Application of Artificial Neural Networks in Forecasting a Standardized Precipitation Evapotranspiration Index for the Upper Blue Nile Basin. Water. 2020;**12**(643):1-19. DOI: 10.3390/

w12030643www.mdpi.com/journal/water

[15] Morid S, Smakhtin V, Bagherzadeh K. (2007) Drought forecasting using artificial neural networks and time series of drought indices. International Journal of Climatology. 2007;**27**:2103-2111

[16] Weerasinghe HDP, Premaratne HL, Sonnadara DUJ. Performance of neural networks in forecasting daily precipitation using multiple choices. J. Natn. Sci. Foundation Sri Lanka. 2010;**38**(3):163-170

[17] Mathugama SC, Peiris TSG. Critical evaluation of dry spell research. International Journal of Basic and Applied Sciences IJBAS-IJENS. 2011;**11**(06):153-160

[18] NiMet NWP Unit with GCRF African SWIFT Project. Sub Seasonal - to- Seasonal (S2S) CLIMATE Forecast over West African Sub-Region with Special Emphasis on Nigeria. Abuja, Nigeria: NiMet-SWIFT Publication; 2020. pp. 1-11

[19] Nigerian Meteorological Agency. Overview of the 2020 Seasonal Rainfall Prediction, (prepared by J. I. Adamu). Abuja: Nigerian Meteorological Agency Publication; 2020. pp. 1-40

[20] Dee DP, Uppala SM, Simmons AJ, Berrisford P, Poli P, Kobayashi S, et al. The ERA-Interim reanalysis: Configuration and performance of the data assimilation system. Quart. J. Roy. Meteorol. Soc. 2011;**137**(656):553-597

[21] Huffman GJ, Bolvin DT, Nelkin EJ, Wolff DB, Adler RF, Gu G, et al. The TRMM multisatellite precipitation analysis (TMPA): quasi-global, multiyear, combined-sensor precipitation estimates at fine scales. Journal of Hydrometeorology. 2007;**8**(1):38-55

[22] Domonkos P, Coll J. Homogenisation of temperature and precipitation time series with ACMANT3: method description and efficiency tests. International Journal of Climatology. 2017;**37**:1910-1921

[23] Adeyeri OE, Laux P, Lawin AE, Ige SO, Kunstmann H. Analysis of hydrometeorological variables over the transboundary Komadugu-Yobe basin. West Africa: Journal of Water and Climate Change. 2020;1339-1354. Doi: 10.2166/wcc.2019.283. (http://creativecommons.org/licenses/by/4.0/)

[24] Benoit P. The start of the growing season in Northern Nigeria. Agricultural Meteorology. 1977;**18**:91-99

[25] Odekunle TO. Determining rainy season onset and retreat over Nigeria from precipitation amount and number of rain days. Theoretical and Applied Climatology. 2006;**83**:163-201

[26] Nema MK, Khare D, Chandniha SK. Application of artificial intelligence to estimate the reference evapotranspiration in sub-humid Doon valley. Applied Water Science. 2017;7:3903-3910. DOI: 10.1007/s13201-017-0543-3

[27] Djaman K, O'Neill M, Diop L, et al. 2019 Evaluation of the Penman-Monteith and other 34 reference evapotranspiration equations under limited data in a semiarid dry climate. Theoretical and Applied Climatology. 2019;**137**:729-743. DOI: doi. 10.1007/s00704-018-2624-0

[28] Paredes P, Fontes JC, Azevedo EB. *et al.* 2018 Daily reference crop evapotranspiration in the humid environments of Azores islands using reduced data sets: accuracy of FAO-PM temperature and Hargreaves-Samani methods. Theoretical and Applied Climatology (2018);134:595-611. https://doi.org/10.1007/s00704-017-2295-2.

[29] Douguedroit A. 1987 The variations of dry spells in marseilles from 1865 to 1984. International Journal of Climatology. 1987;7:541-551

[30] Raymond F, Ullmann A, Camberlin P, Drobinski P, Chateau Smith C. Extreme dry spell detection and climatology over the Mediterranean Basin during the wet season. Geophysical Research Letters. 2016;**43**:7196-7204. DOI: 10.1002/2016GL069758

[31] Raymond F, Ullmann A, Camberlin P, Oueslati B, Drobinsky P. 2018 Atmospheric conditions and weather regimes associated with extreme winter dry spells over the Mediterranean basin. Clim. Dynam. 2018;**50**:4437-4453. DOI: 10.1007/s00382- 017-3884-6

[32] Serra C, Lana X, Burgueno A, Martinez MD. 2016 Partial duration series distributions of the European dry spell lengths for the second half of the twentieth century. Theoretical and Applied Climatology. 2016;**123**:63-81

[33] Tramblay Y, Hertig E. 2018 Modelling extreme dry spells in the Mediterranean region in connection with atmospheric circulation. Atmospheric Research. 2018;**202**:40-48

[34] Lobell DB, Hammer GL, Chenu K, Zheng B, Mclean G, Chapman SC. 2015 The shifting influence of drought and heat stress for crops in northeast Australia. Global Change Biology. 2015;**21**:4115-4127. DOI: doi.org/10.1111/gcb.13022

[35] Allen CD, Breshears DD, McDowell NG. On underestimation of global vulnerability to tree mortality and forest die off from hotter drought in the Anthropocene. Ecosphere. 2015;**6**(8):1-55. DOI: 10.1890/ES15-00203.1

[36] Anderegg WRL, Klein T, Bartlett M, Sack L, Pellegrini AFA, Choat B, et al. 2016 Meta-analysis reveals that hydraulic traits explain cross-species patterns of drought-induced tree mortality across the globe. P. Natl. Acad. Sci. USA. 2016;**113**:5024-5029

[37] McMahon TA, Peel MC, Lowe L, Srikanthan R, McVicar TR. 2013 Estimating actual, potential, reference crop and pan evaporation using standard meteorological data: a pragmatic synthesis. Hydrology and Earth System Sciences. 2013;**17**:1331-1363. DOI: doi.org/10.5194/hess-17-1331-2013

[38] Rivoire P, Tramblay Y, Neppel L, Hertig E, Vicente-Serrano SM. Impact of the dry-day definition in Mediterranean extreme dry-spell analysis Nat. Hazard Earth Syst. Sci. 2019;**19**:1629-1638. DOI: hess-19-1629-2019

[39] Engelbrecht BMJ, Dalling JW, Perason TRH, Wolf RL, et al. Short dry spells in the wet season increase mortality of tropical pioneer seedlings. Oecologia. 2006;**148**(2):258-269

[40] Sawa BA, Adebayo AA. Effects of Pentad dry spells on the yield of some crops in the semi-arid eco-climate region of Northern Nigeria. The Zaria Geographer. 2018;**19**(1):49-60 [Accessed: 12 February 2020]

[41] Luk KC, Ball JE, Sharma A. An application of neural networks for rainfall forecasting. Mathematical and Computer Modelling. 2001;**33**(6-7):683-693

[42] Zhang G, Patuwo BE, Hu MY. Forecasting with artificial neural network: The state of the art. International Journal of Forecasting. 1998;**14**(1998):35-62. DOI: 10.1016/S0169-2070(97)00044-7

[43] Ripley BD. Statistical aspects of neural networks network and chaos - statistical and probabilistic aspects

Chapter 2. In: Barn-dorff-Nielsen OE, Jensen JL and Kendall WS, editors. Chapman k Hall, London: Networks and Chaos: Statistical and Probabilistic Aspects. 1993. pp. 40-123

[44] Cheng B, Titterington DM. Neural Networks : A review from a statistical perspective. Statistical Science. 1994;**9**(1):2-30

[45] Hornik K, Stinchcombe M, White H. Multilayer feedforward networks are universal approximators. Neural Networks. 1989;**2**:359-366

[46] Hornik K. Some new results on neural network approximation. Neural Networks. 1993;**6**:1069-1072

[47] Cybenko G. Approximation by superpositions of a sigmoidal function. Math. Control Signal Systems. 1989;**2**:303-314. DOI: 10.1007/BF02551274

[48] Affandi AK, Watanabe K. Daily groundwater level fluctuation forecasting using soft computing technique. Nature and Science. 2007;**5**(2):1-10

[49] Gupta MM, Jin L and Homma, N. Static and Dynamic Neural Networks: From Fundamentals to Advanced Theory. Hoboken, New Jersey, John Wiley & Sons, Inc; 2003. pp. 1-722

[50] Haykin S. Neural Networks: A Comprehensive Foundation. 2nd. ed. Upper SaddleRever, New Jersey: Prentice Hall; 1999

[51] Akpan VA, Hassapis GD. Nonlinear model identification and adaptive model predictive control using neural networks. ISA Transactions. 2011;**50**(2):177-194. DOI: 10.1016/j.isatra.2010.12.007 Epub 2011 Feb 1. PMID: 21281932

[52] R Core Team. R: A Language and Environment for Statistical Computing. Vienna, Austria: R Foundation for Statistical Computing; 2017. Available from: https://www.R-project.org/

[53] Fritsch S and Guenther F. 2016. guenther@leibniz-bips.de, German Research Foundation (DFG: http://www.dfg.de) under grant scheme PI 345/3-1

[54] Riedmiller M. *Rprop - Description and Implementation Details*. Technical Report. Karlsruhe, Germany: University of Karlsruhe; 1994

[55] Riedmiller M, Braun H. A direct adaptive method for faster backpropagation learning: The RPROP algorithm. In: Proceedings of the IEEE International Conference on Neural Networks (ICNN). San Francisco, CA, USA: IEEE; 1993. pp. 586-591. DOI:10.1109/ICNN.1993.298623

[56] Anastasiadis AD, Magoulas GD, Vrahatis MN. *New globally convergent training scheme based on the resilient propagation algorithm*. Neurocomputing. 2005;**64**:253-270

[57] Vamsidhar E, Varma KVSRP, Rao PS, Satapati R. Predicting rainfall using backpropagation neural network model. International Journal on Computer Science and Engineering. 2010;**02**(04):1119-1121

[58] Dubey AD. Artificial neural network models for rainfall prediction in Pondicherry. International Journal of Computer Applications (0975-8887). 2015;**120**(3):30-35

[59] Kumar A, Kumar A, Ranjan R, Kumar S. A rainfall prediction model using artificial neural network. In: Control and Syst. Graduate Research Colloq. (ICSGRC). 2012. pp. 82-87

[60] Barron AR. A comment on "Neural networks: A review from a statistical perspective". Statistical Science. 1994;**9**(1):33-35